

# Measurements of Density and Speed of Sound of JP-10 and a Comparison to Rocket Propellants and Jet Fuels

Stephanie L. Outcalt\* and Arno Laesecke

Materials Measurement Laboratory, Thermophysical Properties Division, Experimental Properties of Fluids Group, National Institute of Standards and Technology, 325 Broadway, Boulder, Colorado 80305-3337, United States

**ABSTRACT:** Densities of the missile fuel JP-10 were measured with two vibrating-tube densimeters. The combined range of the data is from 270 to 470 K, with pressures up to 30 MPa. The speed of sound in the fuel was measured with a propagation time method at ambient pressure from 278.15 to 343.15 K. The results for density and speed of sound at ambient pressure were combined to obtain the adiabatic compressibility. Correlations are reported that represent the temperature and pressure dependence of the experimental density data within their estimated uncertainty. The properties of JP-10 are compared to those of other previously measured jet and rocket fuels.

## 1. INTRODUCTION

JP-10 is essentially exotetrahydrodicyclopentadiene ( $C_{10}H_{16}$ ; CAS number 2825-82-3; molar mass = 136.23 kg kmol<sup>-1</sup>). It is also known as *exo*-tricyclo(5.2.1.0<sup>2,6</sup>)decane (TCD). It has a very low freezing point (194 K), which has made it the only fuel used for air-breathing missiles in the United States at the present time.<sup>1</sup> Because of its high thermal stability, high energy density, low cost, and widespread availability, JP-10 is being investigated as a fuel to be used in pulse-detonation engines (PDEs), where operational temperatures and pressures are very high (1000–2500 K and 0.1–10 MPa).<sup>2</sup> Because of their potential to produce a higher thermodynamic efficiency, PDEs are being explored for lightweight, low-cost, fuel-efficient space propulsion systems and other flight systems.<sup>3</sup>

The measurements reported here are part of a project to characterize fuels and rocket propellants<sup>1,4–9</sup> to develop physical property models that will aid in the optimal use of the fluids and efficient engine design. Densities of the missile fuel JP-10 have been measured in the temperature range from 270 to 470 K, with pressures to 30 MPa. The speed of sound was measured at ambient pressure from 278.15 to 343.15 K. Density and speed of sound are necessary to develop Helmholtz free energy formulations for thermodynamic properties to provide a framework to predict those equilibrium properties of a fluid that have not yet been determined. The properties of JP-10 measured in this work are put in context of the properties of rocket propellants RP-1 and RP-2 and a Jet-A that we have characterized previously.<sup>10</sup>

## 2. SAMPLE CHARACTERIZATION

The JP-10 sample measured in this work was provided by the Fuels Branch of the Air Force Research Laboratory, Wright–Patterson Air Force Base, OH. The sample composition was analyzed in our laboratory with a gas chromatography–mass spectrometry method. The analysis showed the major constituents to be JP-10 [TCD, *exo*-tetrahydrodicyclopentadiene, 96.5%], adamantane (1.0%), and an endoisomeric modification of TCD (2.5%). Details of the chemical analysis of the sample are given by Bruno et al.<sup>1</sup>

To meet the U.S. Military Specification MIL-DTL-87107D<sup>11</sup> for JP-10, the fuel composition must be a minimum of 98.5% of the *exo* isomer. Therefore, unlike the jet fuels and rocket propellants that we have measured previously,<sup>10,12</sup> JP-10 is not a complex mixture but rather a simple fluid where the major “impurity” is typically the *endo* isomer. Its macroscopic properties can thus be related to the molecular characteristics of its main constituent, TCD. To supplement our measurements and aid in their interpretation, we have included in this work a computational study of this compound to elucidate its molecular size, shape, and charge distribution. The equilibrium geometry of TCD and the electrostatic potential around the molecule were determined by *ab initio* calculations in the Hartree–Fock approximation with 6-311+G\*\* polarization basis sets.<sup>13,14</sup> This level of approximation to solve the Schrödinger equation is sufficient for visualization purposes. Quantitative calculations of thermochemical properties of TCD have been carried out by Hudzik et al.,<sup>15</sup> who used density functional theory and considerably higher level composite computational chemistry methods. Figure 1 shows the molecular structure of TCD in terms of a surface of constant electron density at 0.002 electrons au<sup>-3</sup>, with 1 atomic unit = 5.292 nm being the Bohr radius of hydrogen.<sup>16,17</sup> Electron density is a measure of the probability of an electron being present at a certain location, and the isodensity surface shown contains approximately 99% of a molecule. This surface may appear to represent similar information as portrayed in conventional space-filling models that are based on the space that molecules occupy in solid phases. However, isoelectron density surfaces are more realistic because they are smooth and represent molecules as soft and deformable entities instead of assemblies of hard spheres. This is important to understand the roles of attractive and repulsive forces in molecular interactions as well as that of polarizability. An additional and unique advantage of computation-based graphics of molecular structures is that charge distributions across molecules can be visualized. In Figure 1, the

Received: November 18, 2010

Revised: January 20, 2011

Published: February 14, 2011



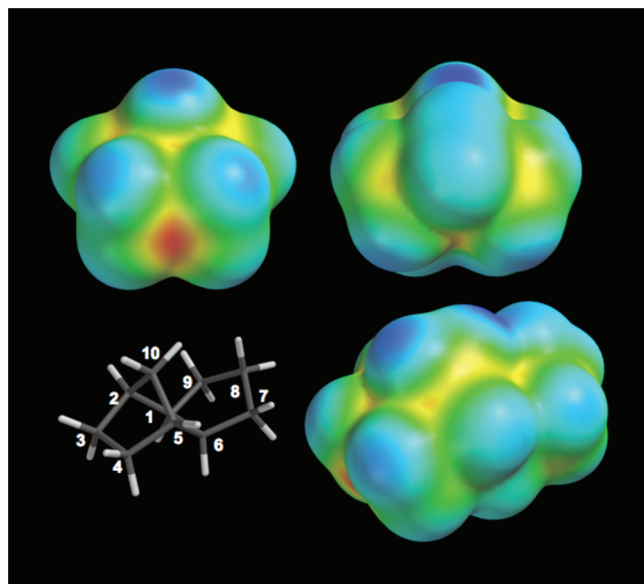


**Figure 1.** Visualization of the molecular size, shape, and charge distribution of TCD. The electrostatic potential is color-mapped onto an electron density isosurface at the level of 0.002 electrons  $\text{au}^{-3}$  (with 1 atomic unit = 5.292 nm being the Bohr radius of hydrogen). This surface represents approximately 99% of a molecule. The color scale ranges from red (negative charge) to blue (positive charge). The molecule is shown in two frontal views along its longitude (top row) and a spatial view (bottom row), where the tube model provides orientation about the positions of the carbon and hydrogen atoms. Most of the outside of the molecule is charged positively, with the exception of a negatively charged region between carbons 3 and 4.

**Table 1.** Density, Speed of Sound, and Adiabatic Compressibility of JP-10 Measured in the Density and Sound Speed Analyzer<sup>a</sup>

temperature <i>T</i> (K)	JP-10		
	density, $\rho$ ( $\text{kg m}^{-3}$ )	speed of sound, $w$ ( $\text{m s}^{-1}$ )	adiabatic compressibility, $\kappa_s$ ( $\text{TPa}^{-1}$ )
278.15	947.3	1490.9	474.9
283.15	943.4	1469.2	491.1
288.15	939.5	1447.7	507.9
293.15	935.6	1426.6	525.2
298.15	931.7	1405.8	543.1
303.15	927.7	1385.2	561.8
308.15	923.8	1364.9	581.1
313.15	919.9	1344.8	601.1
318.15	916.0	1325.0	621.8
323.15	912.1	1305.5	643.4
328.15	908.1	1286.1	665.7
333.15	904.2	1267.0	688.9
338.15	900.2	1248.1	713.1
343.15	896.3	1229.6	738.0

<sup>a</sup> The ambient pressure during the measurements was 0.083 MPa.

electrostatic potential is color-mapped onto the isoelectron density surface with a color scale ranging from red (negative charge) to blue (positive charge). This rendition is the first method that makes polarity visible and, thus, facilitates the understanding of the

contributions of electrostatic forces to intermolecular interactions. These contributions can range from weak attractions to hydrogen bonds, molecular associations, and ionic bonds. The charge distribution across the TCD molecule is rather uniform, as indicated by the computed dipole moment of 0.06 debye. However, the visualization provides more details. Because of the lower electronegativity of the hydrogen atoms, most of the outside of the TCD molecule is partially positively charged, while a negatively charged region is seen between carbons 3 and 4. The work reported here puts these characteristics of molecular size, shape, and charge distribution in context to the measured macroscopic properties of density and speed of sound.

### 3. EXPERIMENTAL SECTION

Two apparatuses were used to perform the density measurements presented here. Both instruments employ vibrating-tube sensors, but they have different temperature and pressure ranges. Their calibration and operating procedures have been described previously in the context of our measurements of methyl- and propylcyclohexane.<sup>18</sup> A density and sound speed analyzer (DSA 5000, Anton Paar Corp.) was used to determine these properties at ambient atmospheric pressure (on average 0.083 MPa at the elevation of 1633 m of Boulder, CO). Temperature scans were programmed in the units of the instrument from 343.15 to 278.15 K in decrements of 5 K. The instrument was calibrated with air and deionized water at 293.15 K. The reproducibility of reference values for the density and sound speed of water at 293.15 K to within 0.01% was checked before and after measurements of the fuel samples to ensure that one sample had been removed completely before another one was injected. The density and speed of sound were measured on the same aliquot of the test liquid JP-10 that remained in the instrument during an entire temperature scan. The relative standard deviation of the repeated density measurements was lower than 0.002%; note that the quoted uncertainty by the manufacturer is 0.1% for both the density and speed of sound determination. However, as a result of recent measurements, we conservatively estimate the expanded uncertainty of the speed of sound determinations to be 0.3% (coverage factor  $k = 2.3$ ) and 0.04% ( $k = 2.3$ ) for the density determinations.<sup>6</sup> Compressed liquid density measurements were made with the fully automated densimeter of Outcalt and McLinden<sup>19</sup> over the temperature range of 270–470 K and up to pressures of 30 MPa. The sample was measured along isotherms from highest to lowest pressure at each temperature from 270 to 470 K in 20 K increments. The densimeter was calibrated with propane<sup>20</sup> and toluene,<sup>21</sup> and the expanded uncertainty in density is calculated to be 0.81  $\text{kg m}^{-3}$  ( $k = 2$ ).

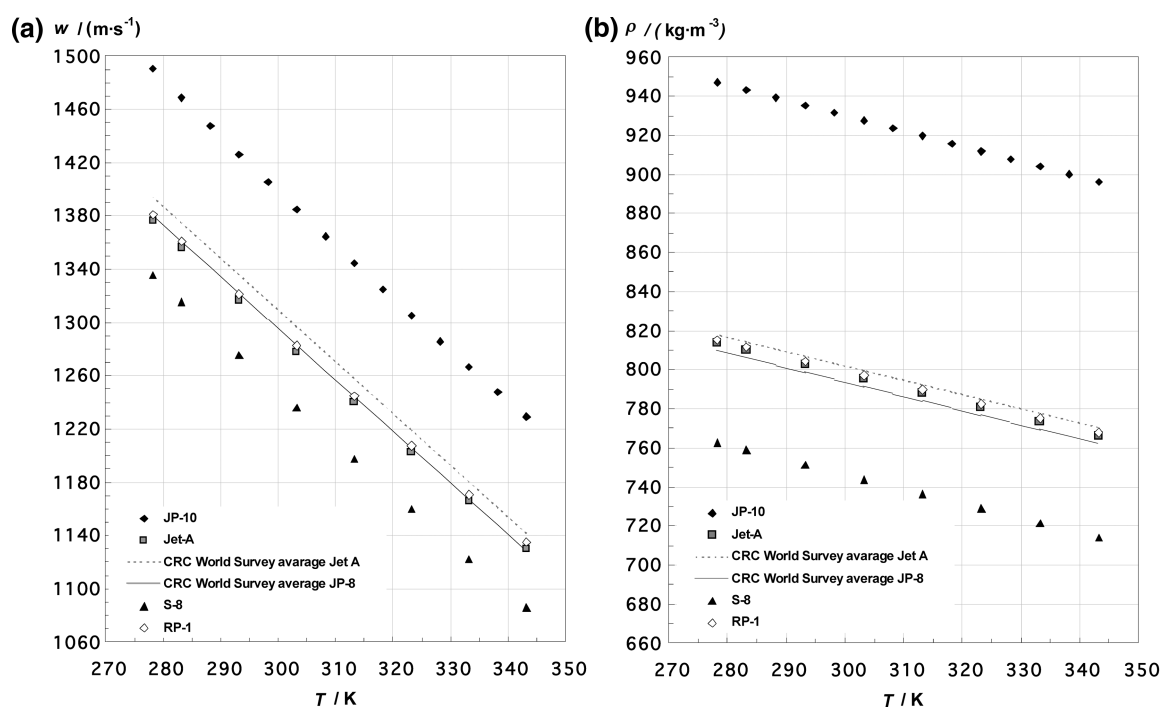
### 4. RESULTS

Table 1 lists values of density, speed of sound, and derived adiabatic compressibilities for the JP-10 sample at the local atmospheric pressure of 0.083 MPa from 278.15 to 343.15 K. Adiabatic compressibilities were calculated from the measured densities and speeds of sound according to the thermodynamic relation

$$\kappa_s = -(\partial V / \partial p)_s / V = 1 / (\rho w^2) \quad (1)$$

where  $V$  denotes volume,  $p$  is the pressure,  $\rho$  is the density, and  $w$  is the speed of sound. The subscript  $s$  indicates “at constant entropy”.

The temperature dependencies of the JP-10 data for speed of sound and density at ambient pressure are illustrated in panels a and b of Figure 2. For comparison, data of a previously measured Jet-A,<sup>10</sup> the synthetic fuel S-8,<sup>10</sup> and rocket propellant RP-1<sup>12</sup> are



**Figure 2.** (a) Measured speed of sound data and (b) measured and extrapolated density data of JP-10 compared to those of other jet fuels reported previously in refs 10 and 12 and the correlations for (a) speed of sound and (b) density of average Jet-A and JP-8 from the CRC World Survey<sup>22</sup> as a function of temperature at ambient pressure.

**Table 2.** Compressed Liquid Densities of JP-10 Measured in the High-Pressure Vibrating-Tube Densimeter along Isotherms from 270 to 470 K<sup>a</sup>

270 K		290 K		310 K		330 K		350 K		370 K	
pressure, $p$ (MPa)	density, $\rho$ ( $\text{kg m}^{-3}$ )	pressure, $p$ (MPa)	density, $\rho$ ( $\text{kg m}^{-3}$ )	pressure, $p$ (MPa)	density, $\rho$ ( $\text{kg m}^{-3}$ )	pressure, $p$ (MPa)	density, $\rho$ ( $\text{kg m}^{-3}$ )	pressure, $p$ (MPa)	density, $\rho$ ( $\text{kg m}^{-3}$ )	pressure, $p$ (MPa)	density, $\rho$ ( $\text{kg m}^{-3}$ )
29.98	968.8	29.99	954.9	30.00	940.6	29.99	926.5	30.00	912.8	30.00	899.1
25.00	966.4	25.00	952.3	25.00	937.8	25.00	923.5	25.00	909.5	25.00	895.4
20.00	964.0	19.99	949.6	20.00	934.8	20.00	920.3	19.99	906.0	20.00	891.6
15.00	961.5	15.00	946.9	15.00	931.8	14.99	917.0	15.00	902.4	15.00	887.7
10.00	958.9	10.00	944.1	10.01	928.7	10.00	913.6	10.00	898.7	9.99	883.6
5.00	956.3	5.00	941.2	4.99	925.5	4.99	910.1	5.00	894.8	5.00	879.3
4.00	955.7	4.00	940.6	4.00	924.8	3.99	909.3	4.00	894.0	3.99	878.4
2.99	955.2	2.99	940.0	2.99	924.2	2.99	908.6	3.00	893.1	3.00	877.5
2.00	954.7	1.99	939.4	2.00	923.5	1.99	907.9	2.00	892.3	1.99	876.5
1.00	954.1	0.99	938.8	0.98	922.8	1.00	907.1	0.99	891.5	1.00	875.6
0.49	953.8	0.50	938.5	0.50	922.5	0.49	906.8	0.49	891.0	0.50	875.2
0.083	953.6	0.083	938.3	0.083	922.2	0.083	906.4	0.083	890.7	0.083	874.8

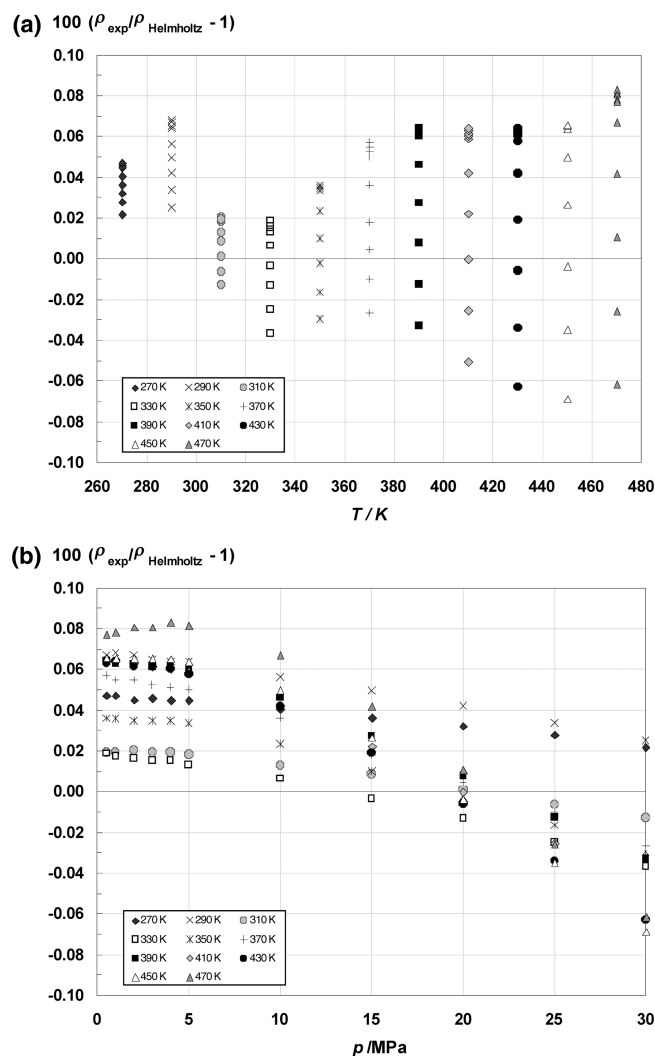
  

390 K		410 K		430 K		450 K		470 K	
pressure, $p$ (MPa)	density, $\rho$ ( $\text{kg m}^{-3}$ )	pressure, $p$ (MPa)	density, $\rho$ ( $\text{kg m}^{-3}$ )	pressure, $p$ (MPa)	density, $\rho$ ( $\text{kg m}^{-3}$ )	pressure, $p$ (MPa)	density, $\rho$ ( $\text{kg m}^{-3}$ )	pressure, $p$ (MPa)	density, $\rho$ ( $\text{kg m}^{-3}$ )
29.99	885.3	30.00	871.4	29.99	857.5	29.99	843.6	30.00	829.9
25.00	881.3	25.00	867.1	24.99	852.8	25.00	838.6	25.00	824.3
20.01	877.2	20.00	862.6	20.00	847.9	19.99	833.1	20.00	818.4
14.99	872.9	15.00	857.8	15.00	842.7	14.99	827.4	14.98	812.0
9.99	868.3	10.00	852.8	9.99	837.1	9.99	821.2	10.00	805.1
5.00	863.5	5.00	847.5	4.99	831.1	5.00	814.4	4.99	797.4
3.99	862.5	3.99	846.3	4.00	829.8	3.99	813.0	4.00	795.8

Table 2. Continued

390 K		410 K		430 K		450 K		470 K	
pressure, $p$ (MPa)	density, $\rho$ (kg m <sup>-3</sup> )	pressure, $p$ (MPa)	density, $\rho$ (kg m <sup>-3</sup> )	pressure, $p$ (MPa)	density, $\rho$ (kg m <sup>-3</sup> )	pressure, $p$ (MPa)	density, $\rho$ (kg m <sup>-3</sup> )	pressure, $p$ (MPa)	density, $\rho$ (kg m <sup>-3</sup> )
2.99	861.5	3.00	845.2	3.00	828.6	3.00	811.6	2.99	794.1
1.99	860.5	2.00	844.1	2.00	827.3	2.00	810.1	2.00	792.5
1.00	859.4	1.00	842.9	0.99	825.9	1.00	808.6	1.00	790.7
0.50	858.9	0.50	842.3	0.49	825.2	0.49	807.8	0.49	789.8
0.083	858.5	0.083	841.8	0.083	824.7	0.083	807.2	0.083	789.1

<sup>a</sup> Values extrapolated to 0.083 MPa are indicated in italics.



**Figure 3.** Deviations of measured compressed liquid densities from the Helmholtz equation given by Bruno et al.<sup>1</sup> as a function of (a) temperature and (b) pressure.

shown as well. Also included in both panels are the respective correlations for Jet-A and JP-8 properties from the CRC World Survey.<sup>22</sup> The Jet-A data shown were taken on a sample that was a mixture of five different Jet-A fuels that were blended to be generically representative of the large composition variations in Jet-A fuels. The RP-1 data is representative of both RP-1 and RP-2 that we have measured, because the properties of the two fluids in the temperature range shown are so similar that they are within the

**Table 3.** Parameters of the Correlation (eq 2) for the Density of JP-10 at Ambient Pressure of 0.083 MPa and Temperatures from 270 to 470 K

parameter	JP-10	
	value	standard deviation
$\beta_1$ (kg m <sup>-3</sup> )	293.822	0.079
$\beta_2$	0.504584	$6.7 \times 10^{-5}$
$\beta_3$ (K)	621.385	0.047
$\beta_4$	0.574121	$8.4 \times 10^{-5}$

size of the symbol representing RP-1. There are several available formulations of RP-1, but only two formulations of RP-2. The data referenced here for RP-1 and RP-2 were taken on the samples for which preliminary surrogate models were published by Huber et al.<sup>23</sup> Figure 2a shows that S-8 has the lowest speed of sound of all of the fuels considered here, while the JP-10 sample measured in this work has by far the largest values. The same is true for the densities shown in Figure 2b. These panels indicate how different the properties of JP-10 are compared to the other fuels. The high density and speed of sound of JP-10 result from the close packing of carbon atoms in the more globular TCD molecule, while the other fuels consist mainly of aliphatic and aromatic hydrocarbons, whose molecular structures entail greater excluded volumes that reduce the macroscopic density. Ambient pressure density and speed of sound of JP-10 reported here were also compared to calculations using the Helmholtz free energy formulation given by Bruno et al.<sup>1</sup> The average absolute deviation (AAD) for density was 0.02%, and the AAD for speed of sound was 0.04%. Both of these average deviations are within the estimated uncertainties of the experimental data reported here.

Table 2 lists measured density values of compressed liquid JP-10 from 270 to 470 K with pressures to 30 MPa. It includes density values extrapolated to the local ambient pressure of 0.083 MPa at each temperature. The extrapolated data were obtained by fitting second-order polynomials to the isothermal densities at pressures less than or equal to 10 MPa and then calculating the densities at 0.083 MPa from the polynomials. This extrapolation was performed to examine the consistency of the compressed-liquid data with the measurement results at ambient pressure from the density and sound-speed analyzer. This consistency will be addressed in the Correlation of Data section below. Deviations of our compressed liquid density data from the Helmholtz free energy formulation for JP-10 given by Bruno et al.<sup>1</sup> are shown in panels a and b of Figure 3 as a function of the temperature and pressure, respectively. The formulation represents all of our data with an AAD of 0.04%, i.e., within their



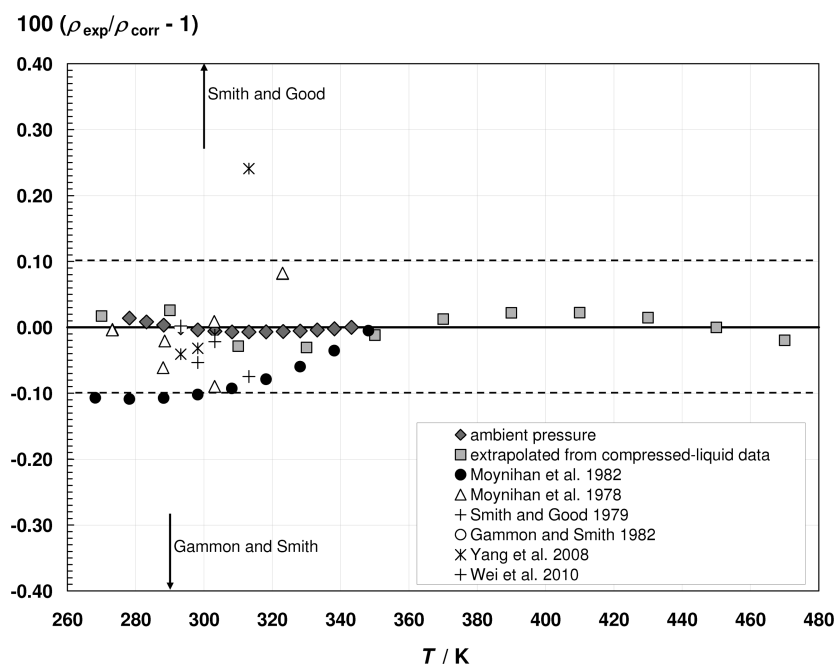


**Figure 4.** Deviations of measured and extrapolated ambient pressure density data of JP-10 from the correlation (eq 2). Also shown are deviations of literature data.

**Table 4.** Parameters of the Correlation (eq 3) for the Density of JP-10 in Terms of Temperature and Pressure

parameter	JP-10	
	value	standard deviation
$C$	$79.18232 \times 10^{-3}$	$1.9 \times 10^{-4}$
$D_1$	417.1	1.1
$D_2$	-370.4	1.1
$D_3$	86.24	0.30

experimental uncertainty. However, the deviations increase systematically with increasing temperature and change signs from positive to negative with increasing pressure along isotherms (with the exception of those at 270 and 290 K). The systematic deviations result from the fact that the Helmholtz free energy formulation was fitted not only to the density data of this work but also simultaneously to the sound speed data as well as other properties of JP-10 from the literature.

## 5. CORRELATION OF DATA

Density measurements at ambient pressure and values extrapolated to 0.083 MPa from experimental compressed-liquid data as reported in Table 2 were combined and correlated with a Rackett-type equation to check the repeatability of the instruments and the consistency of our data in the temperature range of 270–470 K. The equation is written as

$$\rho = \beta_1 \beta_2 - \left( 1 + \left( 1 - \frac{T}{\beta_3} \right)^{\beta_4} \right) \quad (2)$$

Table 3 lists the correlation parameters for eq 2 and their standard deviations as obtained by nonlinear least-squares regression. In Figure 4, this correlation serves as the baseline to

compare the data at ambient pressure to the extrapolated values. It can be seen that both our measured and extrapolated data agree within the bounds of the estimated uncertainty of the density measurements, shown as the dashed line. A survey of the literature revealed six sets of ambient pressure density data.<sup>24–29</sup> Deviations of those data are included in Figure 3. The majority of the data agree with ours within our experimental uncertainty. Data with deviations of more than  $\pm 0.4\%$  are those of Smith and Good<sup>27</sup> and Gammon and Smith.<sup>26</sup>

Density data for the compressed liquid were correlated with a Tait equation similar to that by Dymond and Malhotra<sup>30</sup> of the form

$$\rho(T, p) = \frac{\rho_{\text{ref}}(T, p_{\text{ref}})}{1 - C \ln \left( \frac{p + D(T)}{p_{\text{ref}} + D(T)} \right)} \quad (3)$$

where  $\rho_{\text{ref}}(T)$  is the temperature-dependent density at the reference pressure  $p_{\text{ref}} = 0.083$  MPa from eq 2. The temperature dependence of the parameter  $C$  was omitted, because it was not needed to fit the data within their experimental uncertainty. The temperature dependence of the Tait parameter  $D(T)$  was expressed by a quadratic polynomial

$$D(T) = D_1 + D_2 T_r + D_3 T_r^2 \quad (4)$$

where  $T_r$  is the absolute temperature  $T$  divided by 273.15 K. Values of the four adjusted parameters in eqs 3 and 4 and their standard deviations are given in Table 4. Panels a and b of Figure 5 show deviations of the measured compressed liquid density data relative to the Tait equation of state. This correlation represents our data with an AAD of 0.015%, which is well within their estimated uncertainty. One advantage of the Tait equation of state is that it can be reliably extrapolated to pressures considerably higher than those to which it was fitted.<sup>18</sup> In the case of JP-10, we expect that extrapolations to pressures of 100 MPa will yield densities with an estimated uncertainty of 0.1%.

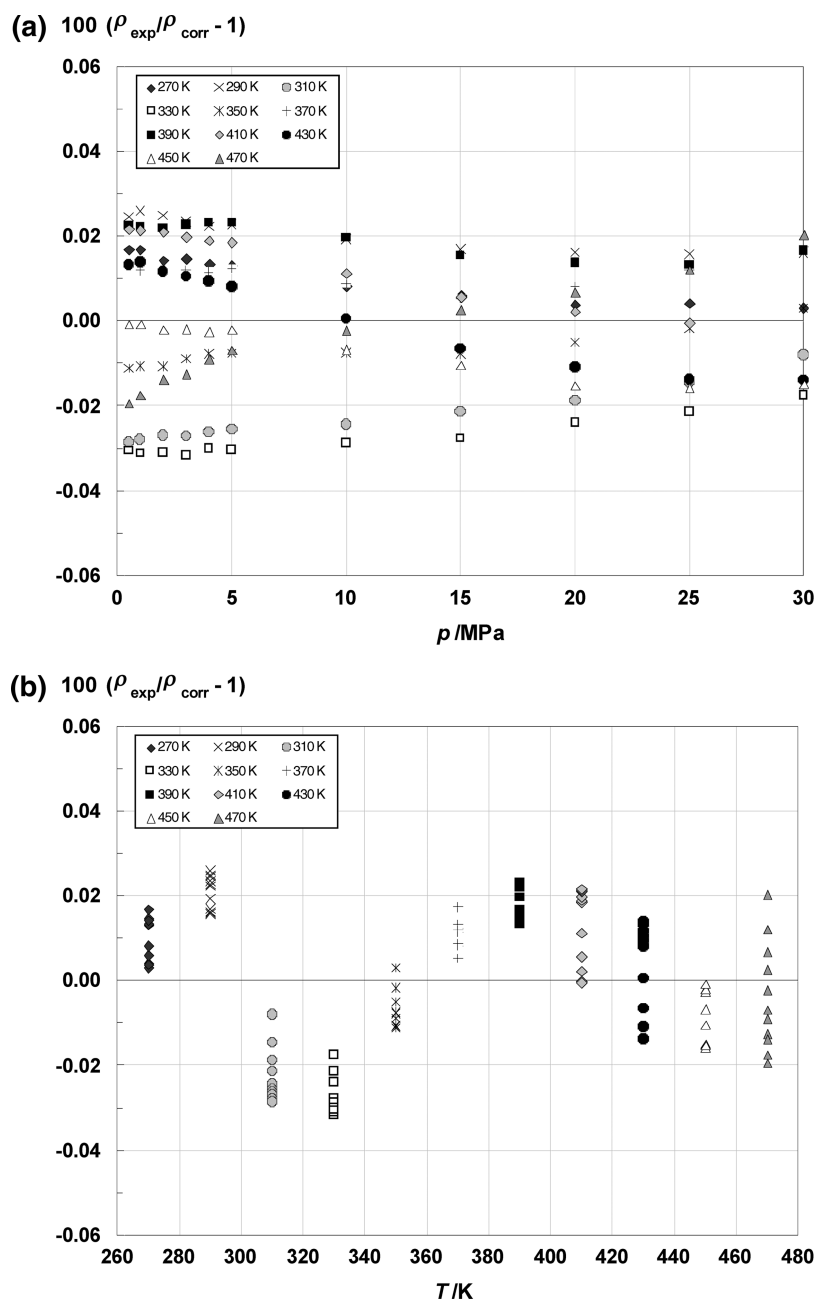


Figure 5. Deviations of density data of compressed liquid JP-10 from the correlation (eqs 3 and 4) as a function of (a) pressure and (b) temperature.

## 6. CONCLUDING REMARKS

In this work, the density and speed of sound of jet fuel JP-10 have been measured at ambient pressure in the temperature range from 278.15 to 343.15 K. No prior measurements of sound speed of this fuel were found in the literature. Density measurements were carried out over a temperature range from 270 to 470 K, with pressures to 30 MPa. The density measurements at ambient pressure support extrapolations of the compressed liquid densities to ambient pressure, which is a prerequisite to developing a correlation of the density data over the entire measurement range. Included correlations of experimental densities represent the data within their estimated uncertainties. The Tait correlation provided here offers an easy to use equation for fitting compressed-liquid density data over large ranges of temperature and pressure.

The measured properties of JP-10 (at ambient pressure) were compared to those of other fuels that were measured previously in this laboratory.<sup>10,12,31</sup> JP-10 has the highest density and speed of sound of the compared fuels. This is consistent with its molecular size, shape, and charge distribution also studied in this work. For instance, on the basis of the *ab initio* calculations described in the Sample Characterization section, the TCD molecule ( $C_{10}H_{16}$ ) has a calculated volume of  $162.4 \text{ \AA}^3$  compared to  $198 \text{ \AA}^3$  of *n*-decane ( $C_{10}H_{22}$ ), which has only six more hydrogens. The tighter packing on the molecular level is reflected in the higher density that was measured in this work. In addition to its high density and speed of sound, JP-10 has other unique properties, such as high thermal stability and high energy density;<sup>2,3</sup> therefore, while in its pure form, it may only have niche applications, it has the potential to

be used as an additive to other fuels to optimize their performance.

A unique property of JP-10 of scientific interest is the extraordinarily wide temperature range of its liquid region from the melting point of 194 K to the critical point at 698 K (where it is thermally unstable<sup>1</sup>). It is known that the length of the vapor pressure curve of a compound reflects the contributions of repulsive and attractive forces to its molecular interaction potential.<sup>32</sup> The shorter the vapor pressure curve, the more repulsive the molecular interactions. Conversely, the long vapor pressure curve of JP-10 indicates that long-range attractive forces play a significant role in its interactions. This unique balance between attractive and repulsive contributions to the force field of JP-10 warrants further investigation that could be benchmarked against the accurate experimental data reported in this work.

## AUTHOR INFORMATION

### Corresponding Author

\*Telephone: 1-303-497-5786. Fax: 1-303-497-5224. E-mail: outcalt@boulder.nist.gov.

## DISCLOSURE

Disclaimer: To describe materials and experimental procedures adequately, it is occasionally necessary to identify commercial products by manufacturers' names or labels. In no instance does such identification imply endorsement by the National Institute of Standards and Technology, nor does it imply that the particular product or equipment is necessarily the best available for the purpose.

## ACKNOWLEDGMENT

We acknowledge the financial support of the Air Force Research Laboratory (MIPR F4FBY5102G001) and valuable discussions with our colleague Dr. Thomas Bruno (NIST, Boulder, CO) during the writing of this paper.

## REFERENCES

- (1) Bruno, T. J.; Huber, M. L.; Laesecke, A.; Lemmon, E. W.; Perkins, R. A. *Thermochemical and Thermophysical Properties of JP-10*; U.S. Department of Commerce: Gaithersburg, MD, 2006; p 66.
- (2) Li, S. C.; Varatharajan, B.; Williams, F. A. Chemistry of JP-10 ignition. *AIAA J.* **2001**, 39 (12), 2351–2356.
- (3) Chenoweth, K.; van Duin, A. C. T.; Dasgupta, S.; Goddard, W. A., III. Initiation mechanisms and kinetics of pyrolysis and combustion of JP-1-hydrocarbon jet fuel. *J. Phys. Chem. A* **2009**, 113 (9), 1740–1746.
- (4) Bruno, T. J.; Laesecke, A.; Outcalt, S. L.; Seelig, H. D.; Smith, B. L. *Properties of a 50/50 Mixture of Jet-A + S-8*; U.S. Department of Commerce: Gaithersburg, MD, 2007; p 32.
- (5) Bruno, T. J.; Huber, M. L.; Laesecke, A.; Lemmon, E. W.; McLinden, M. O.; Outcalt, S. L.; Perkins, R. A.; Smith, B. L.; Widgren, J. A. *Thermodynamic, Transport, and Chemical Properties of "Reference" JP-8*; U.S. Department of Commerce: Gaithersburg, MD, 2010.
- (6) Outcalt, S. L.; Laesecke, A.; Fortin, T. J. Density and speed of sound measurements of 1- and 2-butanol. *J. Mol. Liq.* **2010**, 151, 50–59.
- (7) Smith, B. L.; Bruno, T. J. Improvements in the measurement of distillation curves. 4. Application to the aviation turbine fuel Jet-A. *Ind. Eng. Chem. Res.* **2006**, 46 (1), 310–320.
- (8) Smith, B. L.; Bruno, T. J. Application of a composition-explicit distillation curve metrology to mixtures of Jet-A and S-8. *J. Propul. Power* **2008**, 24 (3), 618–623.
- (9) Widgren, J. A.; Bruno, T. J. Thermal decomposition kinetics of the aviation turbine fuel Jet A. *Ind. Eng. Chem. Res.* **2008**, 47 (13), 4342–4348.
- (10) Outcalt, S.; Laesecke, A.; Freund, M. B. Density and speed of sound measurements of Jet A and S-8 aviation turbine fuels. *Energy Fuels* **2009**, 23, 1626–1633.
- (11) Department of Defense. *Detail Specification Propellant, High Density Synthetic Hydrocarbon Type, Grade JP-10, MIL-DTL-87107D*; Department of Defense: Wright–Patterson Air Force Base, OH, 2006.
- (12) Outcalt, S. L.; Laesecke, A.; Brumback, K. J. Thermophysical properties measurements of rocket propellants RP-1 and RP-2. *J. Propul. Power* **2009**, 25 (5), 1032–1040.
- (13) Hehre, W. J. *A Guide to Molecular Mechanics and Quantum Chemical Calculations*; Wavefunction, Inc.: Irvine, CA, 2003; p 796.
- (14) Gubbins, K. E.; Moore, J. D. Molecular modeling of matter: Impact and prospects in engineering. *Ind. Eng. Chem. Res.* **2010**, 49 (7), 3026–3046.
- (15) Hudzik, J. M.; Asatryan, R.; Bozzelli, J. W. Thermochemical properties of *exo*-tricyclo[5.2.1.0<sup>2,6</sup>]decane (JP-10 jet fuel) and derived tricyclodecyl radicals. *J. Phys. Chem. A* **2010**, 114 (35), 9545–9553.
- (16) Gillespie, R. J.; Popelier, P. L. A. *Chemical Bonding and Molecular Geometry: From Lewis to Electron Densities*; Oxford University Press: New York, 2001; p 268.
- (17) Gillespie, R. J.; Robinson, E. A. Models of molecular geometry. *Chem. Soc. Rev.* **2005**, 34 (5), 396–407.
- (18) Laesecke, A.; Outcalt, S. L.; Brumback, K. J. Density and speed of sound measurements of methyl- and propylcyclohexane. *Energy Fuels* **2008**, 22, 2629–2636.
- (19) Outcalt, S. L.; McLinden, M. O. Automated densimeter for the rapid characterization of industrial fluids. *Ind. Eng. Chem. Res.* **2007**, 46, 8264–8269.
- (20) Lemmon, E. W.; McLinden, M. O.; Wagner, W. Thermodynamic properties of propane. III. A reference equation of state for temperatures from the melting line to 650 K and pressures up to 1000 MPa. *J. Chem. Eng. Data* **2009**, 54 (12), 3141–3180.
- (21) McLinden, M. O.; Splett, J. D. A liquid density standard over wide ranges of temperature and pressure based on toluene. *J. Res. Natl. Inst. Stand. Technol.* **2008**, 113 (1), 29–67.
- (22) Hadaller, O. J.; Johnson, J. M. *World Fuel Sampling Program*; Coordination Research Council: Alpharetta, GA, 2006; CRC Report Number 647.
- (23) Huber, M. L.; Lemmon, E. W.; Ott, L. S.; Bruno, T. J. Preliminary surrogate mixture models for the thermophysical properties of rocket propellants RP-1 and RP-2. *Energy Fuels* **2009**, 23 (6), 3083–3088.
- (24) Moynihan, C. T.; Sasabe, H.; Czaplak, D. S.; Schnaus, U. E. Enthalpies of fusion, freezing points, heat-capacities, densities, and shear viscosities of hydrogenated dimers of norbornadiene and cyclopentadiene. *J. Chem. Eng. Data* **1978**, 23 (2), 107–111.
- (25) Moynihan, C. T.; Sharhriari, M.; Mossadegh, R.; Adel-Hadadi, M.; Boulos, E. N. *Melting Point and  $\nu$  Viscosity Behavior of High Energy Density Missile Fuels*; Catholic University of America: Washington, D.C., 1982; AFWAL-TR-82-2025.
- (26) Gammon, B. E.; Smith, N. K. *Thermodynamics of Organic Compounds*; Bartlesville Energy Technology Center: Bartlesville, OK, 1982; AFOSR-TR-83-0047.
- (27) Smith, N. K.; Good, W. D. Enthalpies of combustion of ramjet fuels. *AIAA J.* **1979**, 17 (8), 905–907.
- (28) Wei, H.; Guo, Y.; Yang, F.; Fang, W.; Lin, R. S. Densities and viscosities of *exo*-tetrahydrodicyclopentadiene + *n*-butanol and *exo*-tetrahydrodicyclopentadiene + *n*-pentanol at temperatures of (293.15 to 313.15) K. *J. Chem. Eng. Data* **2010**, 55 (2), 1049–1052.
- (29) Yang, F. J.; Guo, Y. S.; Xing, Y.; Li, D.; Fang, W. J.; Lin, R. S. Densities and viscosities of binary mixtures of JP-10 with *n*-octane or *n*-decane at several temperatures. *J. Chem. Eng. Data* **2008**, 53 (9), 2237–2240.
- (30) Dymond, J. H.; Malhotra, R. The Tait equation: 100 years on. *Int. J. Thermophys.* **1988**, 9 (6), 941–951.

(31) Outcalt, S.; Laesecke, A.; Brumback, K. J. Comparison of jet fuels by measurements of density and speed of sound of a flightline JP-8. *Energy Fuels* **2010**, *24* (10), 5573–5578.

(32) Anderson, V. J.; Lekkerkerker, H. N. W. Insights into phase transition kinetics from colloid science. *Nature* **2002**, *416* (April 25), 811–815.